

X BAND LINAC MACHINE DESIGN FOR VERY HIGH ENERGY ELECTRON THERAPY

E. Smith^{1,2}, A. Wheelhouse¹, R.M. Jones^{1,2}

¹The Cockcroft Institute of Accelerator Science and Technology, Warrington, UK

²University of Manchester, Oxford Road, Manchester, UK

Abstract

Very high energy electrons (VHEE) are a potential future modality in the field of radiotherapy. They have garnered considerable interest because they possess a unique combination of several properties including: being capable of deep tissue penetration (>30 cm), relative insensitivity to tissue inhomogeneities and being well suited to FLASH therapy. FLASH is the use of ultra-high dose rates which have been shown to reduce cell death in healthy tissue whilst maintaining toxicity to tumours. This paper provides a design for a 250 MeV linac with dose rates exceeding 100 Gy s^{-1} in a 5 cm diameter field. The design is centred on a bi-periodic, $\pi/2$ mode, normal conducting, standing wave, accelerating cavity with a gradient of 80 MV m^{-1} to achieve the compactness required to fit the accelerator in a hospital setting. To this end, 11.9942 GHz X-band technology has been selected which, along with extensive cell geometry optimisation, has produced a shunt impedance of $>100 \text{ M}\Omega \text{ m}^{-1}$ whilst minimising surface electric and magnetic fields.

INTRODUCTION

Very High Energy Electron (VHEE) beams with energies typically ranging from 100 MeV to 250 MeV are an emerging modality in the field of radiotherapy, driven by the following potential benefits. VHEE beams can reach deep seated tumors more effectively than X-rays, the most commonly used modality [1]. VHEE beams are also relatively insensitive to tissue inhomogeneities in the body [2] allowing for more robust treatment planning.

X-ray beams are in general produced by colliding low energy electrons with a tungsten target in a process that converts only 1 % to 2 % of the electrons' energy into usable photons making high dose rates difficult to reach. Ultra High Dose Rates (UHDR), usually defined as $>40 \text{ Gy s}^{-1}$ have been empirically shown to reduce damage to healthy tissue whilst maintaining toxicity to cancerous cells [3]. This "FLASH" therapy widens the therapeutic window and

could be used to reduce required dose fractionation. VHEE beams can also be steered readily by magnetic fields.

One of the primary challenges of delivering VHEE FLASH therapy to patients is the development of an electron linac capable of the required energy and dose rate with a form factor compact enough to fit easily within a hospital setting. Recent advances in high gradient accelerator cavities designed for linear colliders [4] could be used to realize this requirement. The following paper outlines a high level design for an X-band 250 MeV linac operating at a gradient of 80 MV m^{-1} whilst targeting a dose rate of 100 Gy s^{-1} in a circular field 5 cm in diameter.

ACCELERATING CAVITY

The main accelerating cavities of the linac are 25 normal conducting copper structures operating at the X band frequency of 11.9942 GHz. This frequency was chosen over the lower S and C bands more common in radiotherapy to allow for high shunt impedance which becomes particularly important at the high gradients required for compact VHEE machines. For this project a shunt impedance of $100 \text{ M}\Omega \text{ m}^{-1}$ was targeted. The cavities are designed to operate in the $\pi/2$ coupling mode of acceleration because of its inherent stability which is particularly important in medical applications. As is standard for a $\pi/2$ mode accelerator, the cell structure is bi-periodic to reduce the space used by coupling cells however the cells are left on axis to ease the manufacturing cost and complexity of an X-band system. Standing wave fields will be used to prevent fields entering the coupling cells. The electric field distribution for one of the 13.76 cm long optimized 19 cell (10 accelerating and 9 coupling) structures can be seen in Fig. 1. The optimization is detailed below.

The geometry of the cavities was initially designed and tested as a half unit cell which can be seen in Fig. 2. Each accelerating cell is defined by four elliptical arc segments joined by straight line segments which were optimized by a

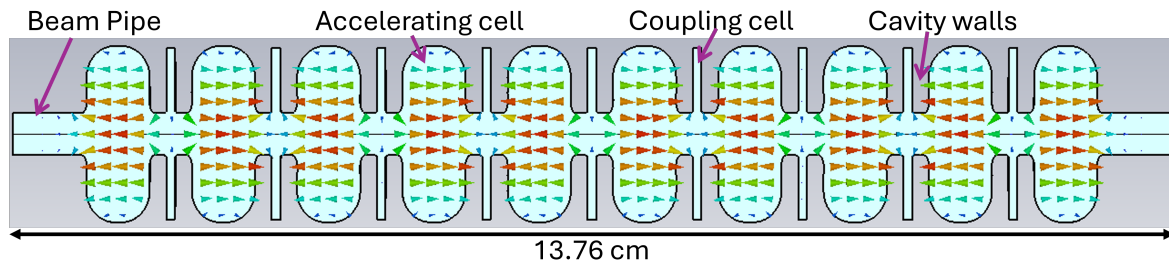


Figure 1: Electric field distribution for the 19 cell $\pi/2$ coupling mode main accelerating cavity simulated in CST.

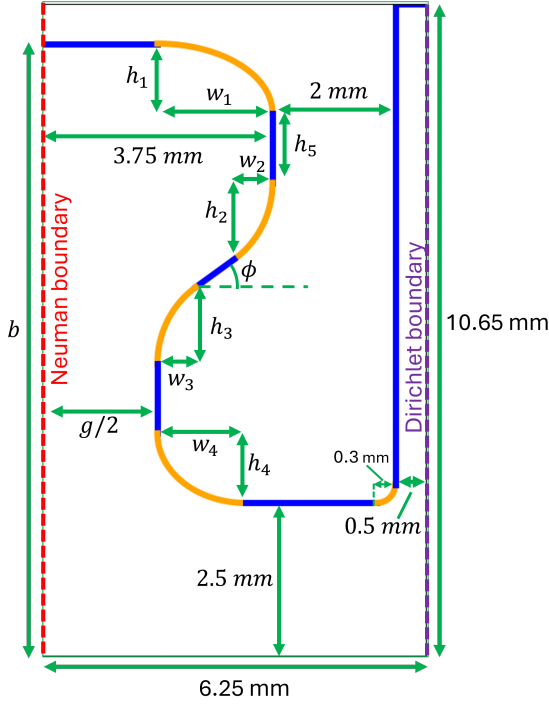


Figure 2: Diagram showing the straight (blue) and elliptical (orange) line segments and their parameters that define the shape of the accelerating cavity unit cell. All straight line segments are perfectly horizontal or vertical except where denoted by angle ϕ .

Non-dominated Sorting Genetic Algorithm (NSGA II) [5,6] in order to minimize the cost function seen in Eq. (1) subject to the ratio between the maximum surface electric field E_{max} and the average accelerating gradient E_{acc} being <2.25 .

$$\frac{H_{max}(\Delta f + 500\text{MHz})}{R_{sh}} \quad (1)$$

where H_{max} represents the maximum surface magnetic field of the cavity, R_{sh} represents the cavity shunt impedance and Δf is the difference between the simulated cavity frequency and the target 11.9942 GHz. The 500 MHz is included to prevent the frequency tuning dominating the optimization. There were 128 generations with population size of 128 simulated across eight hours in Superfish [7]. The optimized values of the 12 geometric parameters are displayed in Table 1.

Table 1: Optimised Cavity Parameters (see Fig. 2)

Parameter	value (mm)	Parameter	value (mm)
h_1	3.693	w_1	3.304
h_2	0.935	w_2	0.004
h_3	0.711	w_3	0.029
h_4	1.516	w_4	0.592
h_5	0.997	ϕ ($^\circ$)	83.595
g	7.428	b	10.421

Electric field distributions of three generations of the genetic algorithm can be seen in Fig. 3.

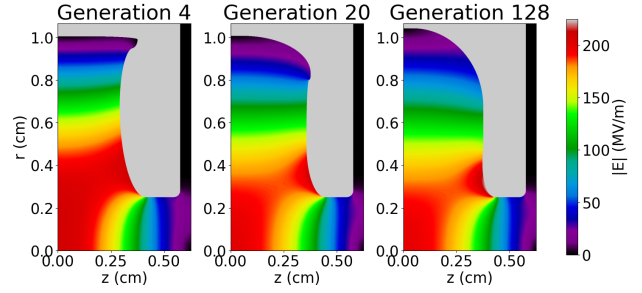


Figure 3: Electric field distribution of three generations of optimization for a half unit cell simulated in superfish.

For a bi-periodic design there are two equally valid $\pi/2$ mode distributions, one in which each of the two cell types are filled with the EM fields. If the two cell types are not tuned to the same frequency, a “stop-band” opens up in the dispersion relation for the cavity as seen in Fig. 4. The data

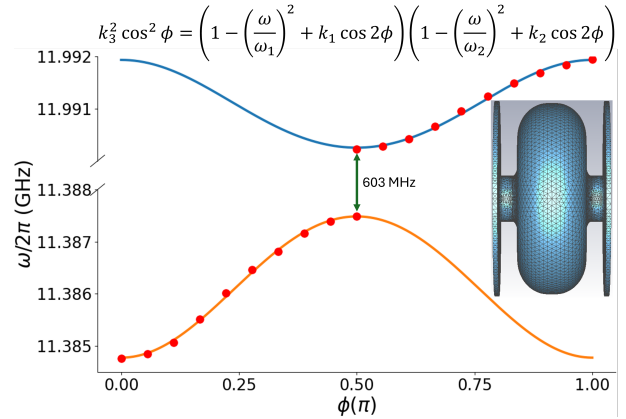


Figure 4: Dispersion relationship for the open band cells simulated in CST. Note the broken axes.

was fit using the capacitively coupled circuit model [8] for a bi-periodic structure which is represented by Eq. (2).

$$k_3^2 \cos^2 \phi = \left(1 - \left(\frac{\omega}{\omega_1} \right)^2 + k_1 \cos(2\phi) \right) \times \left(1 - \left(\frac{\omega}{\omega_2} \right)^2 + k_2 \cos(2\phi) \right) \quad (2)$$

where ω is the angular frequency of the accelerating mode, ω_1 and ω_2 represents the resonant frequency of each cell type, ϕ is the phase advance and k_x is the bandwidth of the coupling between cell types, 1-1 (k_1), 2-2 (k_2) and 1-2 (k_3). This stop band forces the modes in each of the sub bands closer reducing stability. To maximize the spacing between the $\pi/2$ and neighboring modes the accelerating cell and the coupling cell were re-tuned in CST [9] to precisely 11.9942 GHz by increasing the coupling cell radius to 10.16 mm and w_1 to 3.3313 mm (except for the end cells where $w_i = 3.3318$ mm to account for beam pipe field distortions). The key parameters for the tuned cells are shown in Table 2. With the band gap closed, the dispersion relation for the 19 cell cavity was simulated in CST and fit to Eq. (2) as shown in Fig. 5. The band gap between the two $\pi/2$

modes after tuning was only 31 kHz and the neighboring mode spacing was 6.5 MHz.

Table 2: Key Optimization Figures

Parameter	Superfish	CST
R_{sh} ($M\Omega m^{-1}$)	100.50	100.43
H_{max}/E_{acc} (mT/(MV/m))	4.165	4.378
E_{max}/E_{acc}	2.245	2.297
Q factor	7829	7824
frequency (GHz)	11.9927	11.9942

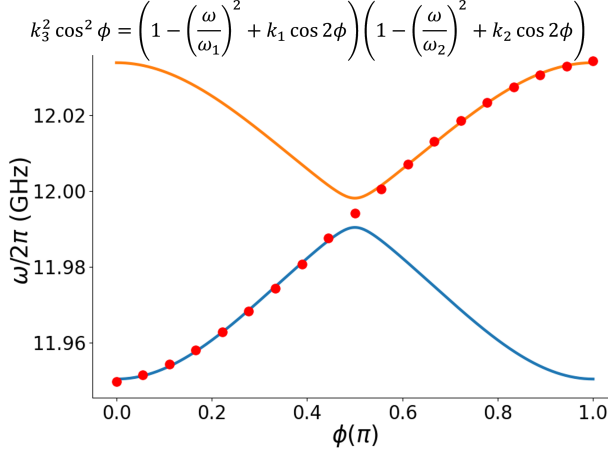


Figure 5: Dispersion relationship for the tuned standing wave coupled cavity linac simulated in CST

POWER REQUIREMENTS

For an 80 MV m^{-1} gradient, 398 kW of power will be dissipated in the cavity walls per half unit cell. For the full 250 MeV target energy, this comes to 199 MW. The only viable RF power supply options for such a high requirement are short pulse klystrons in the $\sim 50 \text{ MW}$ range. The other main draw of power from the system is due to beam loading. Due to the relatively flat dose distribution of VHEE therapy, the approximate average current required to achieve a specified dose rate can be calculated using Eq. (3) [10].

$$I = \frac{D_r \rho A}{L} \quad (3)$$

where D_r (Gy s^{-1}) is the required dose rate, ρ (kg m^{-3}) is the density of water at 1000 kg m^{-3} , A (m^2) is the beam cross sectional area and L ($\text{keV } \mu\text{m}^{-1}$) represents the linear energy transfer of VHEE which is approximately $0.226 \text{ keV } \mu\text{m}^{-1}$. For the case of a dose rate of 100 Gy s^{-1} in a 5 cm diameter field, the required average current is 869 nA, however the more relevant figure is the peak pulse current.

A larger RF pulse length t_{rf} reduces the peak current requirement because the cavity has more time to accelerate the minimum charge per pulse. This in turn lowers the required peak beam power. The beam length is limited however by the time required to fill the cavity to its beam-loaded state. Assuming the beam is only injected once the cavity fills, this beam length t_{beam} is found by numerically solving Eq. (4).

$$t_{rf} - t_{beam} + \tau_f \ln \left(1 - \frac{P_{cavity}}{P_{cavity} + \frac{IV}{f_{rep} t_{beam}}} \right) = 0 \quad (4)$$

where τ_f is the cavity's filling time constant, P_{cavity} is the peak power dissipation by the cavity walls, I represents average beam current, V is the cavity voltage (250 MV) and f_{rep} is the pulse repetition rate.

A SLED type pulse compressor model programmed in MATLAB [11], initially designed for the Compact Linear Accelerator for Research Applications (CLARA) [12], was modified to fit the $1.5 \mu\text{s}$ input pulse typical of 50 MW klystrons. The Broyden-Fletcher-Goldfarb-Shanno (BFGS) [13] algorithm was used to optimize the input waveform in order to minimize the klystron power requirements by balancing the larger power gain achievable from short output pulses with the larger beam power this would cause. The input and output waveforms of this pulse compressor model are seen in Fig 6.

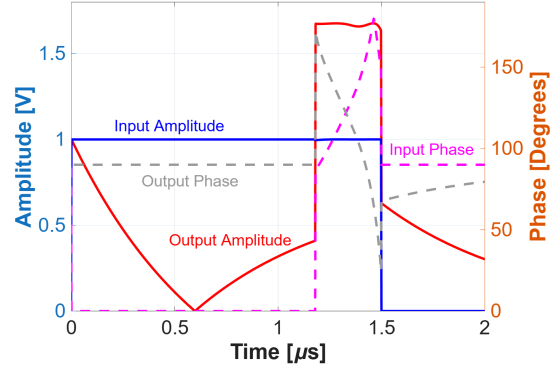


Figure 6: The phase and amplitude wave forms of the input and output of the SLED type pulse compressor

Assuming a 120 Hz repetition rate for the klystrons and that the cavities are critically coupled to the RF input, the optimizer found that the ideal output pulse length was 320 ns of which 82 ns accelerates the beam. This required a peak current of 88 mA and a peak beam power of 22 MW. If we assume $\sim 20\%$ of input power is lost in the input waveguides then the combined power dissipation totals 276 MW. Dividing this by the pulse compressor power gain of 2.79 means the klystrons need to produce 99 MW of power which requires two 50 MW klystrons.

FINAL REMARKS

Outlined in this paper is a design for a 250 MeV bi-periodic axially coupled electron linac for FLASH VHEE therapy. Future studies intend to develop separate side coupled and traveling wave designs and examine whether they offer significant benefits over the current design. A design for an injector, envisaged as a separate standing wave cavity operating at a lower gradient, is also in development. Crucially, the use of X-band frequencies allows this design to be compact, which is critical to the installation and rapid adoption of VHEE FLASH technology.

REFERENCES

- [1] L. Whitmore, R. Mackay I, M. van Herk, J. K. Jones, and R. M. Jones, “Focused VHEE (very high energy electron) beams and dose delivery for radiotherapy applications”, *Sci. Rep.*, vol. 11, no. 1, Jun. 2021.
[doi:10.1038/s41598-021-93276-8](https://doi.org/10.1038/s41598-021-93276-8)
- [2] A. Lagzda *et al.*, “Influence of heterogeneous media on very high energy electron (vhee) dose penetration and a monte carlo-based comparison with existing radiotherapy modalities”, *Nucl. Instrum. Methods Phys. Res., Sect. B*, vol. 482, pp. 70–81, 2020. [doi:10.1016/j.nimb.2020.09.008](https://doi.org/10.1016/j.nimb.2020.09.008)
- [3] M.-C. Vozenin *et al.*, “The advantage of flash radiotherapy confirmed in mini-pig and cat-cancer patients”, *Clin. Cancer Res.*, vol. 25, no. 1, pp. 35–42, Jan. 2019.
[doi:10.1158/1078-0432.CCR-17-3375](https://doi.org/10.1158/1078-0432.CCR-17-3375)
- [4] T. Argyropoulos *et al.*, “Design, fabrication, and high-gradient testing of an X-band, traveling-wave accelerating structure milled from copper halves”, *Phys. Rev. Accel. Beams*, vol. 21, no. 6, p. 061001, Jun. 2018.
[doi:10.1103/PhysRevAccelBeams.21.061001](https://doi.org/10.1103/PhysRevAccelBeams.21.061001)
- [5] K. Deb, A. Pratap, S. Agarwal, and T. Meyarivan, “A fast and elitist multiobjective genetic algorithm: nsga-ii”, *IEEE Trans. Evol. Comput.*, vol. 6, no. 2, pp. 182–197, 2002.
[doi:10.1109/4235.996017](https://doi.org/10.1109/4235.996017)
- [6] J. Blank and K. Deb, “Pymoo: multi-objective optimization in python”, *IEEE Access*, vol. 8, pp. 89497–89509, 2020.
- [7] J. H. Billen and L. M. Young, “POISSON/SUPERFISH on PC Compatibles”, in *Proc. PAC’93*, Washington D.C., USA, Mar. 1993, pp. 790–793.
[doi:10.1109/PAC.1993.308773](https://doi.org/10.1109/PAC.1993.308773)
- [8] E. A. Knapp, B. C. Knapp, and J. M. Potter, “Standing wave high energy linear accelerator structures”, *Rev. Sci. Instrum.*, vol. 39, no. 7, pp. 979–991, Jul. 1968.
[doi:10.1063/1.1683583](https://doi.org/10.1063/1.1683583)
- [9] I. Munteanu and I. Hänninen, “Recent advances in cst studio suite for antenna simulation”, in *Proc. EUCAP 2012*, Prague, Czech, Mar. 2012, pp. 1301–1305, 2012.
[doi:10.1109/EuCAP.2012.6206600](https://doi.org/10.1109/EuCAP.2012.6206600)
- [10] K. L. Small *et al.*, “Evaluating very high energy electron RBE from nanodosimetric pBR322 plasmid DNA damage”, *Sci. Rep.*, vol. 11, no. 1, Feb. 2021.
[doi:10.1038/s41598-021-82772-6](https://doi.org/10.1038/s41598-021-82772-6)
- [11] The MathWorks Inc., OPTIMIZATION TOOLBOX VERSION: 9.4 (R2022B), 2022. <https://www.mathworks.com>
- [12] L. Cowie *et al.*, “An X-Band Lineariser for the CLARA FEL”, in *Proc. IPAC’18*, Vancouver, Canada, Apr.-May 2018, pp. 3848–3851.
[doi:10.18429/JACoW-IPAC2018-THPAL084](https://doi.org/10.18429/JACoW-IPAC2018-THPAL084)
- [13] D. LIU and J. NOCEDAL, “On the limited memory bfgs method for large-scale optimization”, *Math. Program.*, vol. 45, no. 3, pp. 503–528, Dec. 1989.
[doi:10.1007/BF01589116](https://doi.org/10.1007/BF01589116)